Cell. Mol. Life Sci. 64 (2007) 3129 – 3138
1420-682X/07/233129-10
DOI 10.1007/s00018-007-7318-1

Cellular and Molecular Life Sciences

Research Article

A hydrogen-bonding network in mammalian sorbitol dehydrogenase stabilizes the tetrameric state and is essential for the catalytic power

M. Hellgren, C. Kaiser[+], S. de Haij[++], Å. Norberg and J.-O. Höög*

Department of Medical Biochemistry and Biophysics, Karolinska Institutet, 171 77 Stockholm (Sweden), Fax: +468-337-462, e-mail: jan-olov.hoog@ki.se

Received 13 July 2007; received after revision 30 September 2007; accepted 1 October 2007
Online First 20 October 2007

Abstract. Subunit interaction in sorbitol dehydrogenase (SDH) has been studied with *in vitro* and *in silico* methods identifying a vital hydrogen-bonding network, which is strictly conserved among mammalian SDH proteins. Mutation of one of the residues in the hydrogen-bonding network, Tyr110Phe, abolished the enzymatic activity and destabilized the protein into tetramers, dimers and monomers as judged from gel filtration experiments at different temperatures compared to only tetramers for the wild-type protein below 307 K. The determined equilibrium constants revealed a large difference in Gibbs energy (8 kJ/mol) for the tetramer stability between wild-type SDH and the mutated form Tyr110Phe SDH. The results focus on a network of coupled hydrogen bonds in wild-type SDH that uphold the protein interface, which is specific and favorable to electrostatic, van der Waals and hydrogen-bond interactions between subunits, interactions that are crucial for the catalytic power of SDH.

Keywords. Alcohol dehydrogenase, hydrogen-bonding network, Gibbs energy, quaternary structure, sorbitol dehydrogenase, structural zinc.

Introduction

Protein-protein interaction is an intricate cell function where different proteins assemble into complex structures that can create functional units [1]. The diversity and complexity of such protein-protein interactions is difficult to study regardless of method and conditions (*in vivo/vitro/silico*). The functional unit of sorbitol dehydrogenase (SDH, EC 1.1.1.14) is a zinc-dependent homotetrameric enzyme [2] within the protein family of medium chain dehydrogenases/reductases (MDR) with a close relationship to alcohol dehydrogenase (ADH, EC 1.1.1.1) [3]. The mammalian ADHs have a dimeric quaternary structure, whereas most bacterial and yeast ADHs are homotetrameric enzymes like SDH [2, 4–6]. The subunits of SDH are slightly smaller than the mammalian ADH subunits, with a molecular mass of 38 kDa [7]. SDH catalyzes the reversible NAD^+-linked oxidation of different polyols into their corresponding ketoses [8], an enzymatic reaction that is highly pH dependent. SDH is expressed in nearly all tissues but not in the intestinal tract [9], and, together with aldose reductase, SDH metabolically link glucose and fructose in the polyol pathway. These two enzymes have been shown to be coexpressed in several cell lines [10], and

[+] Present address: Biovitrum, 112 76 Stockholm (Sweden)
[++] Present address: Genmab, 3508 AD Utrecht (The Netherlands)
* Corresponding author.

have been extensively studied in connection to vascular dysfunction and pathology in diabetic complications [11].

Information about the location of possible subunit interacting areas in SDH has been revealed from three-dimensional structure determinations of rat and human SDHs [12, 13], as well as an earlier computer modeling study into the structure of horse liver ADH [4]. These studies concluded that two dimers (as in mammalian ADH) form a tetramer in SDH, but details of these interactions have not been investigated further. ADH harbors, beside the active site zinc, also a structural zinc, where four negatively charged cysteine residues coordinate the zinc atom [14]. This structural zinc is conserved in all mammalian ADHs and is crucial for correct folding and activity [15]. In the corresponding area in mammalian SDH the cysteine motif and the structural zinc is missing where amino acid residues 100–110 form a loop region, which interacts with the opposite dimer. Tyr110 at the C-terminal end of this loop region is strictly conserved among analyzed mammalian SDHs and was early identified in subunit interaction by specific labeling [16]. An evolutionary bridge between the two different mammalian structures of ADH and SDH can be observed in silverleaf whitefly SDH and yeast ADH, both of which harbors a structural zinc [5, 17] like mammalian ADHs, but also has a tetrameric quaternary structure as in mammalian SDHs.

In this study *in vitro* and *in silico* methods were utilized to reveal properties of the subunit interactions in SDH. Equilibrium constants *in vitro* between three different quaternary states: monomer, dimer and tetramer in wild-type (wt) SDH and in Tyr110Phe SDH were determined. Differences in Gibbs energy and alterations in the quaternary stability could thus be determined. To further understand subunits interactions in SDH we constructed a scoring energy function that compares the relative enthalpy interaction energy between subunits and amino acid residues 100–110 in the loop region.

Materials and methods

Mutagenesis, expression, purification and characterization. Mutagenesis was performed on a construct of native rat SDH cDNA in expression vector pET12b (Novagen Inc.) [18]. The U.S.E. mutagenesis kit was used (GE Healthcare) to incorporate the desired mutation. All plasmids containing mutated fragments were checked by DNA sequence analyses for correct introduction of base alterations. For expression of recombinant enzymes from the pET12b-constructs, the *E. coli* strain BL21 (DE3) was transformed and cultured in 2 l LB medium supplemented with 100 μg ampicillin/ml. The protein expression was initiated with the addition of 0.4 mM IPTG at an OD of 1.5 and was grown for an additional 2–3 h. Isolation of proteins from the cell lysates were carried out in two steps: DEAE-cellulose (DE-52, 2.6×20 cm column; Whatman) in 0.1 M Tris-HCl, pH 8.0 and a gel filtration step with a HiLoad Superdex 200 (16/60 prep grade; GE Healthcare), 10 mM Tris-HCl, pH 8.0, 0.2 M NaCl. Typical yields of homogenous recombinant proteins were about 3 mg and 15 mg/l culture for the mutant and native SDH, respectively. The elution volume for proteins from the HiLoad Superdex 200 was calibrated with a gel filtration standard kit (13.7–2000 kDa; Sigma-Aldrich) and ADH2 (80 kDa). The homogenous tetrameric SDH fractions from the second gel filtration purification step were collected and used for enzyme activity and further stability experiments. The temperature of the HiLoad Superdex column was regulated with circulating water. To assay for activity, a spectrophotometer (Hitachi U-3000) was used, monitoring the production of NADH at 340 nm, with a mixture containing 50 mM sorbitol, 2.4 mM NAD^+, 0.1 mM glycine/NaOH, pH 10.0. The kinetic constants, K_m and k_{cat}, for sorbitol and xylitol were determined with non-linear regression analysis at steady state under *in vitro* conditions of 0.1 M glycine/NaOH, pH 10.0, 1.0 mM NAD^+ and substrate concentration up to ten times K_m for wt SDH; for ethanol the tested substrate concentrations were 1.0 mM and 100 mM. Tyr110Phe SDH did not show a measurable activity at any stage of purification even at protein concentration of 0.1 mg/ml. The purity of the isolated proteins was verified by SDS-polyacrylamide gel electrophoresis.

Mass spectrometry. Protein bands were excised manually from the SDS/PAGE gels and digested using a MassPREP robotic protein handling system (Waters). Gel pieces were washed, alkylated and digested with trypsin [19]. The tryptic peptide extracts from in-gel digestion were mixed at 1:1 (v/v) with a saturated solution of α-cyano-4-hydroxy cinnamic acid and dried on a standard steel target plate followed by MALDI-TOF mass spectroscopy (Voyager DE Pro, Applied Biosystems). Mass peaks were identified with the software PeptideMass [20].

Circular dichroism spectrometry. Circular dichroism spectra were recorded on protein samples in 20 mM potassium phosphate buffer, 150 mM NaCl, pH 7.6. The concentration of the samples ranged between 0.2 and 1.0 mg/ml. Spectra were recorded from 260 to 198 nm at a step resolution of 0.1 nm and at a scanning speed of 5 nm/min a Jasco CD spectrometer. Wt and

Tyr110Phe SDHs were treated with urea up to 5 M to record the denaturing effect with circular dichroism analysis.

Gibbs energy and apparent equilibrium binding constants. The change in Gibbs energy when passing between two states in a reversible process at constant pressure and temperature is equal to the sum of the heat and work taken up by the system. We have the following relation for changes in Gibbs energy.

$$\Delta G = \Delta H - T\Delta S = \Delta G^0 + RT \times \ln(K) \quad (1)$$

Changes in Gibbs energy can be calculated *in vitro* or *in silico* (Eq. 1). ΔH represents the enthalpy change in the system, ΔS represents the entropy change in the system, T is the temperature, R is the universal gas constant and K is the reaction quotient. At equilibrium, the equilibrium constant (K'^0) is calculated from the fraction of reactants/products ([A] × [A]/[AA]) between the quaternary states, which is used to calculate the standard transformed Gibbs energy ($\Delta G'^0$) of the reaction at specified *in vitro* conditions of temperature, ionic strengths and pH:

$$\Delta G_{eq} = 0 \Rightarrow \Delta G'^0 = -RT \times \ln(K'^0) = -RT \times \ln([A] \times [A]/[AA]) \quad (2)$$

The change in Gibbs energy ($\Delta G'^0$) in the gel filtration experiments is calculated from the equilibrium constant (K'^0) with Eq. 2, after 60 min of incubation at *in vitro* conditions of 10 mM Tris-HCl, pH 8.0, 0.2 M NaCl, 0.1 mg/ml isolated protein and at temperatures 277–317 K. The difference in Gibbs energy between wt SDH and Tyr110Phe SDH at each temperature is given by:

$$\Delta\Delta G'^0 1 = \Delta G'^0 1^{wt} - \Delta G'^0 1^{Tyr110Phe} \quad (3)$$

$$\Delta\Delta G'^0 2 = \Delta G'^0 2^{wt} - \Delta G'^0 2^{Tyr110Phe} \quad (4)$$

Eq. 3 gives the change in Gibbs energy of the mutation between the monomeric and dimeric states and Eq. 4 gives the change in Gibbs energy of the mutation between dimeric and tetrameric states.

Enthalpy calculations and scoring energy function. For energy calculations the ICM version 2.7 was used (Molsoft LLC) with ECEPP/3 molecular mechanics forcefield [21–23]. The structures of human SDH (pdb entry 1PL7), silverleaf whitefly SDH (pdb entry 1e3j) and *Thermoanaerobacter brokii* ADH (TbADH, pdb entry 1YKF) were obtained from the database RCSB and hydrogen atoms were added and followed by a local energy minimization (ICM). All energy calculations were performed on the human SDH structure (from pdb entry 1PL7) due to its higher resolution at the subunit interfaces than in the determined rat SDH structure. The root mean square distance between c-alpha in a comparison from a structural alignment of a single subunit from human and rat SDH was calculated to 1.0 Å (ICM) and between human and silverleaf whitefly SDH it was 1.2 Å (ICM). Complete Gibbs free energy calculations from *in silico* computations with explicit water can be performed with molecular dynamics simulations, but because of computational complexity it is more suitable for smaller systems than studied here. For our purposes a simplified scoring energy function was constructed that compared the relative enthalpy binding energy between subunits and amino acid residues. The electrostatic energy was calculated (ICM) with a distant dependent function. Here we denoted the enthalpy binding energy as the non-covalent interaction in the form of hydrogen bonds, electrostatic and van der Waals energies. The enthalpy binding energy between two subunits (A to D or B to C) to form one complex, i.e., dimer structure, was calculated and this energy was labeled DS (Dimer Score). All other enthalpy binding energies (score energies) were set relative to this DS defined value (Eq. 5). The following formulas were used to compare score energies between subunits A, B, C and D and specific residues in human SDH.

$$DS = E(A\_D) = E(C\_B) = 1 \quad (5)$$

$$TS = E(A\_B) + E(A\_C) + E(B\_D) + E(C\_D) \quad (6)$$

$$BS = N \times E(A(X)\_C(Y)) / TS \quad (7)$$

$$RS = N \times E(A(X)\_C)) / TS \quad (8)$$

TS (Tetramer Score) is the score energy for the formation of one tetramer (Eq. 6). BS (Bond Score) is the relative strength of a single bond between two residues in the formation of a tetramer complex compared to TS (Eq. 7). RS (Residue Score) is the relative strength of the interaction between one residue in one subunit and all other residues in the reverse subunit compared to TS, where N is the number of bonds per tetramer (Eq. 8). In this study the entropy part of Gibbs energy in Eq. 1 is excluded from our scoring energy function, and thereby no absolute values of Gibbs energies are given. Furthermore, the scoring energy function does not include solvent-protein and solvent-solvent interactions. Water molecules, the solvent, often compete with internal protein-protein hydrogen bonds, but can also mediate protein-protein hydrogen bonds. The formation and breaking of hydrogen bonds between water and protein is important for both the stability as well as the catalytic activity of proteins. Hydrogen bonds

```
                                    *           *   *                                                  *
Protein  Species                          100       Tyr110Phe 120                                             T/D  Zn
                                ßßßß  ßß      αααtt 333 tt ßßtt                      tt     t ßßßßß333ßß
SDH      Human               90 RVAIEPGAPRENDEFCKMGRYNLSPSIFFCAT---------------------PPDDGNLCRFYKHNAAFCY 140   T    - 
SDH      Rat                    RVAIEPGVPREINEFCKIGRYNLTPSIFFCAT---------------------PPDGGNLCRFYKHSADFCY       T    - 
SDH      Whitefly               RVAVEPGVPCRRCQFCKEGKYNLCPDLTFCAT---------------------PPDDGNLARYYVHAADFCH       T    Z 
SDH      Yeast                  RVALEPGIPDRFSPEMKEGRYNLDPNLKFAAT---------------------PPFDGTLTKYYKTMKDFVY      (T)  (-)
SDH      S. haemolyticus        RVAIEPGEPCRECEYCKSGQYNLCPHMEFMAT---------------------PPYDGAFCEYVSHPADFLY      (T)  (Z)
ADH      T. brokii              RVVVPAITPDWRTSEVQRGYHQHSGGMLAGWK------------------FSNVKDGVFGEFFHVNDADMNL       T    - 
ADH      C. beijerinckii        RVIVPCTTPDWRSLEVQAGFPQHSNGMLAGWK------------------FSNFKDGVFGEYFHVNDADMNL       T    - 
ADH1     Yeast                  AGIKWLNGSCMACEYCELGNESNCPHA-DLSG---------------------YTHDGSFQQYATADAVQAA       T    Z 
ADH1     Rat                    KVIPLFSPQCGKCRICKHPESNLCCQTKNLTQPKGALLDGTSRFSCRGKPIHHFISTSTFSQYTVVDDIAVA       D    Z 
ADH1B1   Human               88 KVIPLFTPQCGKCRVCKNPESNYCLKN-DLGNPRGTLQDGTRRFTCRGKPIHHFLGTSTFSQYTVVDENAVA 157   D    Z 
                                ßßßß         αααα tt    tt           tt    ßßßttßßßß  ttt   ß ßßßßß333ßß
                                            100                   120                 140
                                         Z  Z  Z       Z
```

Figure 1. Alignment of amino acid residues in the region 90–140 in sorbitol dehydrogenases (SDHs) and alcohol dehydrogenases (ADHs). The numbering at top (90–140) refers to human SDH and at the bottom (88–157) refers to human ADH1B1. The local secondary structure information, as determined from 3D structures of human SDH and human ADH1B1, is marked for β-sheets (β), α-helices (α), 3_{10}-helices (3) and turns (t). The hydrogen-bonding network residues in the region are labeled (*) and the mutated residue Tyr110Phe SDH is marked. The quaternary structure is given in the T/D column as tetramer (T) or dimer (D). Proteins with structural zinc are marked with Z, as are the cysteine residues that coordinate the zinc ion in some of the proteins, see bottom line. There are no high resolution structures available for yeast and *Staphylococcus haemolyticus* SDH, therefore the two last columns are in parentheses for those sequences.

forms and breaks spontaneously at room temperature making the stability of specific bonds difficult to determine. In the x-ray-resolved crystal of human SDH, 1157 oxygen atoms from water molecules were resolved. The enthalpy energy contribution of the water molecules is of significance, but in the enthalpy energy scoring function used we simplified and focused on the specific protein-protein enthalpy interaction. However, this simplified scoring energy function can be used to recognize important binding regions and possibly identify key amino acid residues in protein-protein interaction.

Results

Recombinant rat SDH was mutated at position 110 to exchange a Tyr for Phe, a residue strictly conserved in all structurally analyzed SDHs (Figs. 1, 2). For subunit interaction studies, the Tyr110Phe SDH was expressed in parallel to wt SDH in *E. coli* and isolated to homogeneity in a two-step procedure. In the ion-exchange chromatography step the two proteins showed identical elution profiles, but in the final gel filtration step Tyr110Phe SDH was divided into several fractions. The homogenous tetrameric wt SDH and Tyr110Phe SDH fractions from the gel filtration purification step were collected and used for further catalytic activity measurements, circular dichroism analysis and stability experiments. Calibration of the gel filtration column showed that the fractions from Tyr110Phe SDH corresponded to molecular sizes of >300-, 160-, 80- and 40-kDa proteins, which matches the sizes of aggregate, tetrameric, dimeric and monomeric SDH, respectively. These fractions were verified to contain Tyr110Phe SDH with MALDI-TOF mass spectroscopy.

Results *in vitro*. The relative protein concentrations for monomeric, dimeric and tetrameric wt SDH and Tyr110Phe SDH were determined with gel filtration experiments at five different temperatures from 277 to 317 K (Fig. 3). Only the tetrameric state was observed for wt SDH at temperatures below 307 K, while at 307 K and above also dimeric and monomeric states were detected (Fig. 3a). Tyr110Phe SDH was divided into tetramers, dimers and monomers at all temperatures investigated, with the relative amount of tetramers decreasing with increasing temperature (Fig. 3b). The changes in Gibbs energy ($\Delta\Delta G'^{0}$) were calculated by comparison of the equilibrium constants between the different quaternary states in wt SDH and Tyr110Phe SDH. The $\Delta\Delta G'^{0}1$ for the difference in the free energy of monomers and dimers between wt SDH and Tyr110Phe SDH was 1.4 kJ/mol at 307 K and 3.1 kJ/mol at 317 K (Table 1), respectively. The $\Delta\Delta G'^{0}2$ for the difference in free energy of dimers and tetramers between wt SDH and Tyr110Phe SDH was 8.2 kJ/mol at 307 K and 8.1 kJ/mol at 317 K (Table 1), respectively. No enzymatic activity was detectable, even at protein concentrations up to 0.1 mg/ml for Tyr110Phe SDH with the tested substrates (Table 2). The circular dichroism analysis of wt SDH and Tyr110Phe SDH was similar and showed typical patterns of ordered secondary structure. The stability of wt SDH was also studied at high urea concentration where wt SDH was denatured in 5 M urea. Subsequent dilution of the denatured protein to 1 M urea did not result in refolding of the protein as determined from the spectra (data not shown). The

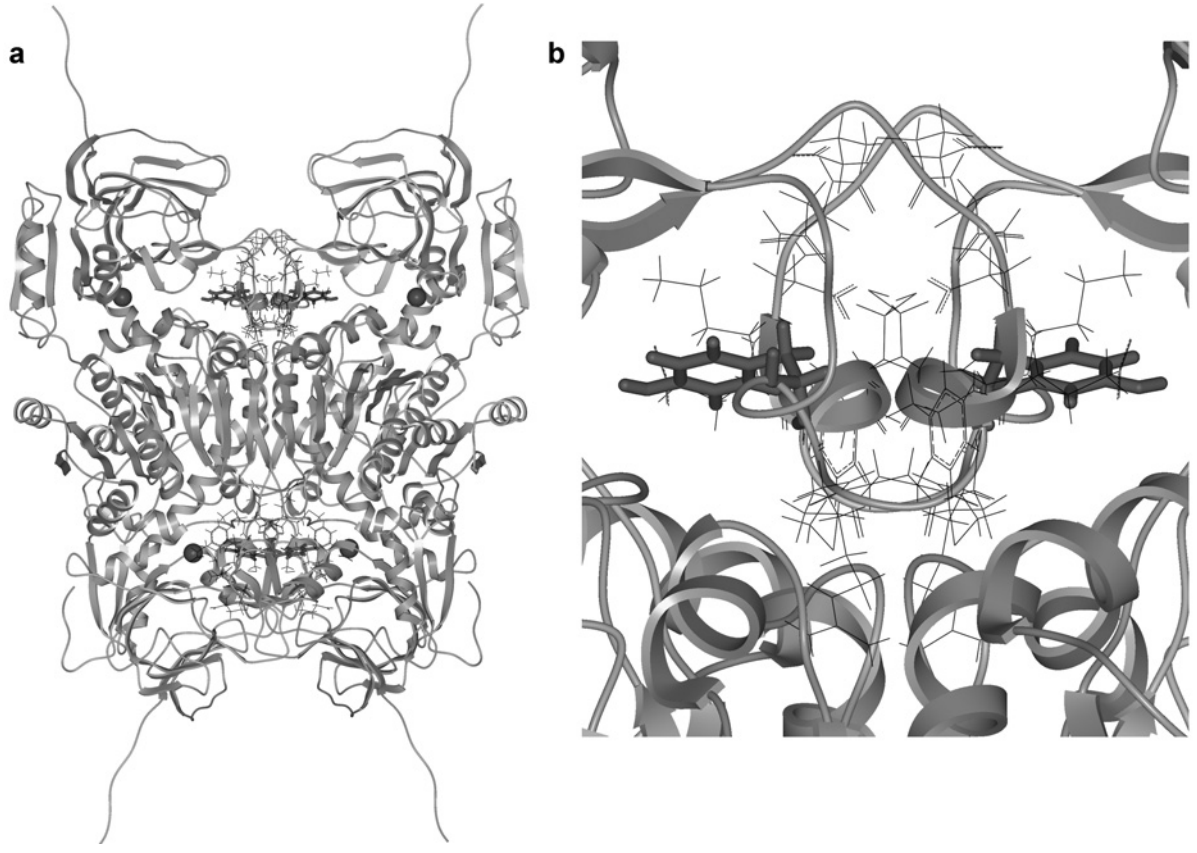

Figure 2. Tetrameric structure of mammalian SDH. In (*a*), Tyr110 is shown in thick style (xstick). (*b*) A close up view of the interaction between subunits in the loop region 100–110.

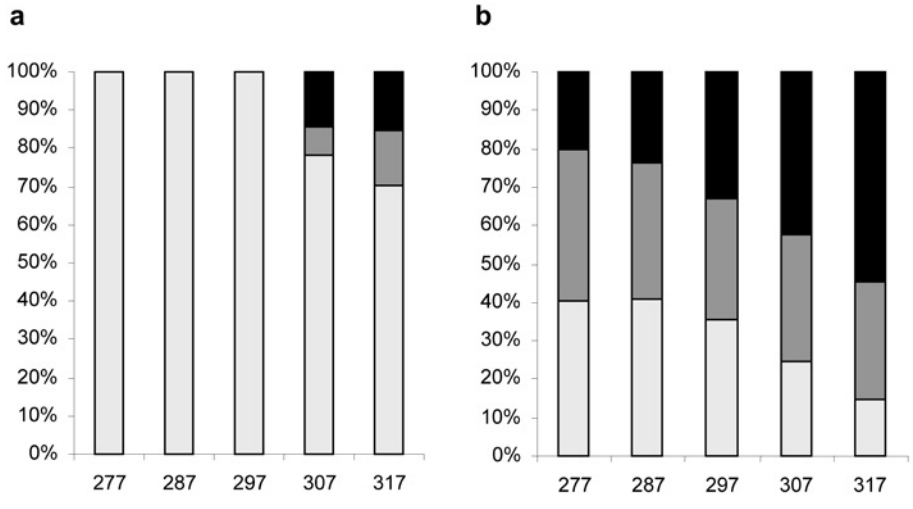

Figure 3. Changes in the relative concentration between the three states in wild-type (wt) SDH and Tyr110Phe SDH induced by temperature shifts. The relative concentration *in vitro* after gel filtration experiments given in percent for the three states – monomeric (black), dimeric (gray) and tetrameric (light gray) in 10 mM Tris-HCl, pH 8.0, 0.2 M NaCl, Protein concentration at incubation 0.1 mg/ml. Five different temperatures were measured from 277 K to 317 K. (*a*) wt SDH, (*b*) Tyr110Phe SDH.

enzymatic activity of native SDH started to decrease at 1.5 M urea and was completely lost at 3.5 M urea. The addition of $ZnSO_4$ in native SDH alleviated the activity loss.

Results *in silico.* The enthalpy between residues and subunits were compared through the constructed scoring energy function (score energy), see Material and methods, and the atomic details behind the interactions were investigated. The score energy between subunits A and D and subunits B and C

Table 1. Stability measurements for wild-type (wt) sorbitol dehydrogenase (SDH) and Tyr110Phe SDH.[a]

Temperature	277 K	287 K	297 K	307 K	317 K
Equilibrium constant	$10^9 \times$ M	$10^9 \times$ M	$10^9 \times$ M	$10^9 \times$ M	$10^9 \times$ M
$K'^0 1^{wt}$	ND	ND	ND	140	110
$K'^0 1^{Tyr110Phe}$	100	130	200	250	350
$K'^0 2^{wt}$	ND	ND	ND	12	20
$K'^0 2^{Tyr110Phe}$	190	170	180	290	420
Gibbs energy	kJ/mol	kJ/mol	kJ/mol	kJ/mol	kJ/mol
$\Delta G'^0 1^{wt}$	ND	ND	ND	40.2 ± 1.0	42.3 ± 0.8
$\Delta G'^0 1^{Tyr110Phe}$	37.2 ± 0.9	37.9 ± 1.6	38.1 ± 1.0	38.8 ± 2.1	39.2 ± 1.3
$\Delta G'^0 2^{wt}$	ND	ND	ND	46.6 ± 0.4	46.8 ± 0.4
$\Delta G'^0 2^{Tyr110Phe}$	35.6 ± 0.7	37.1 ± 0.9	38.4 ± 0.5	38.4 ± 1.6	38.7 ± 2.0
$\Delta\Delta G'^0 1$	ND	ND	ND	1.4	3.1
$\Delta\Delta G'^0 2$	ND	ND	ND	8.2	8.1

[a] In the experiments the equilibrium constant K'^0 (Eq. 2) at different temperatures is given in (M), $K'^0 1$ for monomer to dimer and $K'^0 2$ for dimer to tetramer. The standard transformed Gibbs energy ($\Delta G'^0$) of the reaction is given in kJ/mol ($\pm$ SD) and calculated after four experiments. The change in Gibbs energy in the comparison of the stability of different states (monomeric, dimeric and tetrameric states) by the mutation of wt SDH to Tyr110Phe SDH are given as $\Delta\Delta G'^0$ values. $\Delta\Delta G1'^0$ for the monomer to dimer (Eq. 3), and $\Delta\Delta G2'^0$ for the dimer to tetramer (Eq. 4). ND, not determined because only the tetrameric state in wt SDH could be observed.

Table 2. Catalytic activity determinations for wt SDH and Tyr110Phe SDH.[a]

Substrate	wt K_m (mM)	k_{cat} (min^{-1})	Tyr110Phe K_m (mM)	k_{cat} (min^{-1})
Sorbitol	0.33 ± 0.05	42.6 ± 1.6	–	NA
Xylitol	0.17 ± 0.05	38.1 ± 3.2	–	NA
Ethanol	–	NA	–	NA

[a] Catalytic activity for recombinant wt SDH and Tyr110Phe SDH were measured spectrophotometrically, see Material and methods, with substrate concentrations up to ten times K_m for sorbitol and xylitol, for ethanol the substrate concentration was 1.0 mM and 100 mM. NA, no activity could be measured at protein concentration of 0.1 mg/ml for wt SDH and Tyr110Phe SDH.

showed the highest values, which suggests dimeric formations between these couples (Table 3, Fig. 4). The score energy between the other subunits pairs AB, AC, BD and CD contributes to the tetrameric formation (Table 3). The score energy between two dimer structures (AD or BC) in the formation of a tetramer structure (ADBC) was calculated to be comparable to the score energy in the formation of one dimer structure (Table 3). The entire loop region including amino acid residues 100–110 contribute to 78% of the total score energy in the formation of a tetramer (Tables 4, 5). Tyr110 at the C-terminal end of this loop region forms hydrogen bonds to Glu94 and Asn301 within the same subunit, which stabilizes the entire loop (Fig. 2). Tyr110 as single residue, contribute with only 2% of the total score energy in the formation of a tetramer but the residue is central in the hydrogen-bonding network that links the dimer-dimer interface together (Table 5, Fig. 3). The entire hydrogen-bonding network between the subunits comprises residues Tyr110(subunit A)-Glu94(subunit A)-Tyr140(subunit A)-Lys106(subunit C)-Asn301(subunit A)-Tyr110(subunit A). The positively charged Lys106 is by far the residue that contributes the most to the score energy for the tetramer formation, since it directly interacts with seven other residues in the opposite dimer through three separate hydrogen bonds and with an electrostatic attraction to the negatively charged Glu94 (Tables 4, 5, Fig. 5).

Table 3. Score energy of the relative enthalpy binding energy between subunits in SDH.[a]

Subunit	A	B	C	D
A		0.06	0.18	0.50
B	0.06		0.50	0.18
C	0.18	0.50		0.06
D	0.50	0.18	0.06	

[a] The score energy is calculated according to Eq. 5. The subunits are labeled as in pdb entry 1PL7 to A, B, C and D (see Fig. 1).

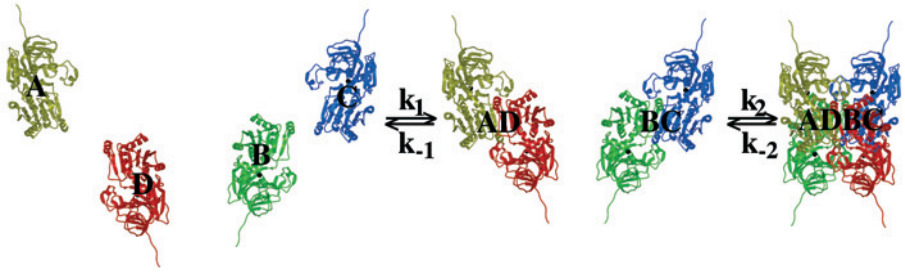

Figure 4. Schematic representation of binding between subunits in SDH. The rate of association and rate of dissociation between subunits are determined by the rate constants. Rate constants between the monomeric and the dimeric state are labeled k_1/k_{-1} and between the dimeric and the tetrameric state k_2/k_{-2}. The subunits are labeled as subunits according to Table 1 and pdb entry 1PL7.

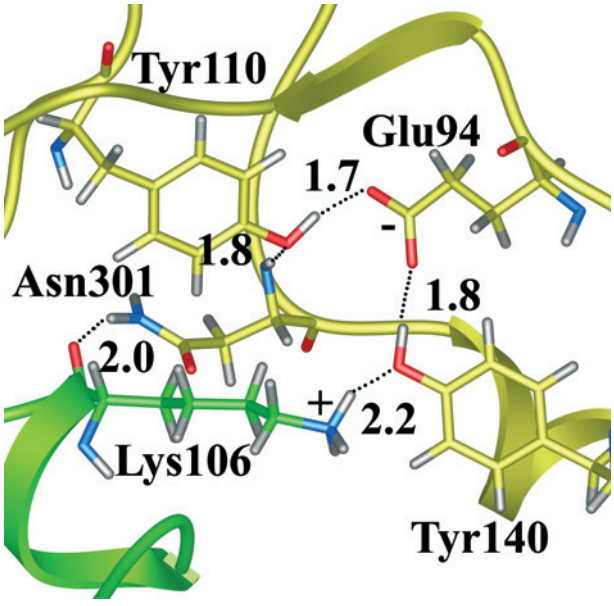

Figure 5. The identified hydrogen-bonding network between subunit A and subunit C in the tetrameric quaternary structure of SDH. Tyr110 in subunit A participates in a chain of hydrogen bonds with residues from subunit A and Lys106 in subunit C. Subunit A are labeled in yellow and subunit C in green. The entire hydrogen network comprise of residues Tyr110(subunit A)-Glu94(subunit A)-Tyr140(subunit A)-Lys106(Subunit C)-Asn301(subunit A)-Tyr110(subunit A). The plus sign (+) shows the positive charge on the Lys106 residue and the minus sign (–) shows the negative charge on the Glu94 residue. There are 30 (per tetramer) resolved water oxygen atoms representing water molecules in the close proximity (<3.0 Å) of the hydrogen-bonding network between the subunits; these water molecules are hydrogen bonded to protein atoms and are of importance for the interaction between subunits, see Material and methods, but have been omitted for the clarity of the picture.

The tetrameric bacterial ADH from TbADH lacks structural zinc like mammalian SDHs, and, from the structural alignment (ICM) with human SDH, the loop formed by amino acid residues 90–100 in the TbADH showed a similar structure to the loop formed by amino acid residues 100–110 in human SDH. The root mean square distance (RMSD) between all structural aligned *c-alpha* atoms of the two tetrameric proteins was calculated to 1.9 Å (ICM). The calculated score energy between subunits in TbADH showed that the loop region consisting of residues 90–100 also contribute to the score energy between subunits in TbADH (data not shown).

Discussion

Protein-protein interactions are essential in many life processes and therefore of wide interest for biochemical and biophysical investigations. Several studies on SDH emphasize its implications for diabetic diseases since the enzyme has a significant role in the polyol pathway in the metabolism of sorbitol [11]. In this study the protein-protein interaction between subunits in SDH was investigated. The properties of wt SDH and Tyr110Phe SDH were studied by a combination of molecular modeling and *in vitro* determination of binding constants, circular dichroism and enzymatic activity. Tyr110 was mutated to Phe to investigate the importance of the loop region of amino acid residues 100–110. The *in vitro* determined equilibrium constant between the monomeric and dimeric state is only slightly changed by the mutation of Tyr110 into Phe in SDH, with a corresponding change in Gibbs energy ($\Delta\Delta G'^{0}1$) of 1–3 kJ/mol (Table 1). However, the stability of the tetrameric state in Tyr110Phe SDH was decreased as compared to wt SDH where the change in Gibbs energy was ($\Delta\Delta G'^{0}2$) 8 kJ/mol (Table 1). This change in Gibbs energy is equivalent to a 20-fold larger equilibrium constant, which clearly shows that the tetrameric quaternary structure is destabilized in Tyr110Phe SDH. Circular dichroism analysis showed that the overall secondary structure was retained between wt SDH and Tyr110Phe SDH, indicating that the mutation primarily affects the dimer-dimer interaction area and not the subunit structure as such. Molecular modeling yielded a hydrogen-bonding network (four per tetramer) that stabilizes the loop consisting of amino acid residues 100–110, which is pivotal for the tetrameric structure (Table 4, Fig. 5).

Table 4. Score energy of bonds between residues in the region 100–110 and other residues.[a]

Subunit 1 (residue)	Subunit 2 (residue)	Distance (Å)	*N*	Type	BS (%)
N101	A137	3.0	4	*vW*	4
	F138	2.4	4	*vW*	4
E103	Y140	2.6	4	*vW*	1
	P304	2.6	4	*vW*	4
K106	**E94**	5.5	4	*el*	6
	G108	2.4	2	*vW*	0.5
	Y110	2.2	2	*vW*	2
	A137	2.0	4	*vW, el, hb*	10
	F138	3.0	4	*vW*	6
	Y140	2.0	4	*vW, el, hb*	9
	N301	2.0	4	*el, hb*	5
M107	G108	2.8	2	*vW*	2

[a] The score energy between subunits ([A to C] or [C to A] or [B to D] or [D to B]) for amino acid residues in the loop (residues 100–110) region. The cut-off distance for displayed residues is 3.0 Å with the exception of the electrostatic interaction between residues Lys106 and Glu94 (5.5 Å). For symmetrical reasons the number of bonds *N* is two or four per tetramer. Distance gives the closest distance between an atom of one subunit (Subunit1) to an atom of another subunit (Subunit2). Type is a classification of the energy for the interaction, where *el* is electrostatic energy, *hb* is hydrogen bond energy and *vW* is van der Waals energy. Bond Score (BS) is the calculated interaction energy between residues and given in percent according to Eq. 7. The residues in the hydrogen-bonding network are labeled in bold.

Table 5. Total score energy for each residue in the region 100–110.[a]

Residue	Type	RS (%)
E100	*el*	4
N101	*vW*	9
D102	–	0
E103	*vW*	2
F104	–	0
C105	*vW*	3
K106	*vW,el,hb*	47
M107	*vW*	6
G108	*vW*	1
R109	*vW*	1
Y110	*vW*	5

[a] The score energy of a single residue from the loop region 100–110 for the binding between subunits ([A to C] or [C to A] or [B to D] or [D to B]). Type is a classification of the energy for the interaction, where *el* is electrostatic energy, *hb* is hydrogen bond energy and *vW* is van der Waals energy. Residue Score (RS) is in relation to the total score energy in the formation of a tetramer and calculated in percent according to Eq. 8.

Here the importance of a correct loop structure is exposed, the rupture of which switches the quaternary structure from tetrameric to dimeric, which is the main overall structural difference between the two mammalian forms of the MDR enzymes, SDH and ADH [2, 4].

Out of 88 loops in interfaces, studied in different dimers and tetramers, about 75% show hydrogen bonds with a secondary structure element from another subunit, with the majority involving main-chain groups [24]. Mammalian dimeric ADHs differ from SDH and tetrameric bacterial ADHs with an insertion of 20 amino acid residues at position 120 in SDH [4]. The tetrameric bacterial TbADH and *Clostridium beijerinckii* ADH are structurally very similar but have a large difference in thermostability. In mutagenesis and molecular modeling studies it was shown that the main source for the difference in stability between the bacterial ADHs was due to critical replacements of residues at the interface areas between subunits [6, 25]. TbADH shows a theme similar to SDH, with a small RMSD of the *c-alpha* atoms compared to SDH. Score energy calculations for the subunits interactions in TbADH showed that the loop region with residues 90–100, which corresponds to the loop region with residues 100–110 in SDH, is also important for subunit interaction. Studies of the other tetrameric ADHs show a pattern similar to that of SDH, e.g., yeast and *E. coli* ADH with a deletion similar to bacterial ADHs, but with a structural zinc atom [5]. The pattern is also present within the SDH enzymes, represented by the structurally determined protein from silverleaf whitefly [17]. This SDH harbors a structural zinc, but with a deleted segment as observed in all SDHs and in most yeast and bacterial ADHs [5]. The interaction between the loop region of residues 100–110 with the region of residues 120–140 is the main contributor (78%) to the score energy between dimers in the formation of a tetramer structure in mammalian SDHs (Table 4). This inter-

action would probably be spoiled by an insertion of 20 amino acid residues at position 120 as in dimeric ADHs. Since all tetrameric ADHs also lack this insertion, this points out the importance of the two regions, residues 90–110 and 120–140, for the stability and binding between subunits in both mammalian SDHs and tetrameric ADHs. The alignment of amino acid sequences from different SDHs and ADHs around the region of the structural zinc in ADH and the deleted segment in SDH clearly shows that the structural zinc is not a determinant for the state of quaternary structure (Fig. 1). The general view from structurally determined SDHs and ADHs is that the early identified deleted segment in sheep SDH and yeast ADH will favor the tetrameric structure [2, 4], which is stressed from the recently determined structures [5, 17, 25]. Further, *in vitro* studies of tetrameric ADHs could verify the importance of these regions for the thermostability of the bacterial ADHs. The loop region with amino acid residues 100–110 is not in close contact with the active site, with the closest atom 14 Å away from the active site zinc atom, which indicates that subunit interaction is critical for the enzymatic function, since no enzymatic activity could be observed in Tyr110Phe SDH. This is in line with similar observations for the bacterial ADHs [6]. Even though a part of Tyr110Phe SDH was eluted as tetramers no enzymatic activity in those fractions was observed, and this proves that not only association between subunits in the tetrameric state is sufficient to induce a catalytic active state. Several site-directed mutagenesis studies have showed that mutations primarily involving changes in the net charge have a significant effect on protein-protein association rates [26, 27], which suggests that the higher stability of wt SDH as compared to Tyr110Phe SDH is probably not caused by a higher rate of association (k_2; Fig. 4). However, electrostatic attraction could still explain part of the change in binding since the mutated residue Tyr110 to Phe destroys the hydrogen-bonding network that links the negatively charged residue Glu94 in one subunit to the positively charged residue Lys106 in another subunit (Table 4, Fig. 5). In line with this we suggest that the decreased stability of the tetrameric state in Tyr110Phe SDH as compared to wt SDH is caused by an increased rate of dissociation (k_{-2}) for the mutant (Fig. 4). The abolished enzymatic function for the tested substrates in Tyr110Phe SDH is probably due to structural changes of the active site due to the altered interaction between subunits. Most likely these structural changes increase the transition state energy barrier for Tyr110Phe SDH, which destroys its catalytic power. The molecular modeling findings of the hydrogen-bonding network together with the *in vitro* experiments of wt SDH and Tyr110Phe SDH gives support to a mechanism where several hydrogen bonds in a network of hydrogen bonds stabilizes the electrostatic attraction between Lys106 and Glu94, which further increasee the binding between subunits. This study thereby shows how a network of coupled hydrogen bonds in SDH upholds a protein interface that is favorable to electrostatic, van der Waals and hydrogen bond interactions between subunits, interactions that are crucial for the catalytic power of SDH.

Acknowledgements. The Karolinska Institutet is acknowledged for financial support.

1 Gavin, A.C., Bösche, M., Krause, R., Grandi, P., Marzioch, M., Bauer, A., Schultz, J., Rick, J.M., Michon, A.M., Cruciat, C.M., Remor, M., Höfert, C. et al. (2002) Functional organization of the yeast proteome by systematic analysis of protein complexes. Nature 415, 141–147.
2 Jeffery, J. and Jörnvall, H. (1988) Sorbitol dehydrogenase. Adv. Enzymol. 61, 47–106.
3 Persson, B., Zigler, J.S. Jr. and Jörnvall, H. (1994) A superfamily of medium-chain dehydrogenases/reductases (MDR). Sub-lines including zeta-crystallin, alcohol and polyol dehydrogenases, quinone oxidoreductase enoyl reductases, VAT-1 and other proteins. Eur. J. Biochem. 226, 15–22.
4 Eklund, H., Horjales, E., Jörnvall, H., Brändén, C.-I. and Jeffery, J. (1985) Molecular aspects of functional differences between alcohol and sorbitol dehydrogenases. Biochemistry 24, 8005–8012.
5 Karlsson, A., El-Ahmed, M., Johansson, K., Shafqat, J., Jörnvall, H., Eklund, H. and Ramaswamy, S. (2003) Tetrameric NAD-dependent alcohol dehydrogenase. Chem. Biol. Interact. 143–144, 239–245.
6 Korkhin, Y., Kalb, J., Peretz, M., Bogin, O., Burstein, Y. and Frolow, F. (1999) Oligomeric integrity – The structural key to thermal stability in bacterial alcohol dehydrogenases. Protein Sci. 8, 1241–1249.
7 Karlsson, C., Jörnvall, H. and Höög J.-O. (1991) Sorbitol dehydrogenase: cDNA coding for the rat enzyme. Variations within the alcohol dehydrogenase family independent of quaternary structure and metal content. Eur. J. Biochem. 198, 761–765.
8 Lindstad, R.I., Koll, P. and McKinley-McKee, J.S. (1988) Substrate specificity of sheep liver sorbitol dehydrogenase. Biochem. J. 330, 479–487.
9 Estonius, M., Danielsson, O., Karlsson, C., Persson, H., Jörnvall, H. and Höög J.-O. (1993) Distribution of alcohol and sorbitol dehydrogenases. Assessment of mRNA species in mammalian tissues. Eur. J. Biochem. 215, 497–503.
10 Hedberg, J.J., Grafström, R.C., Vondracek, M., Sarang, Z., Wärngård, L. and Höög J.-O. (2001) Micro-array chip analysis of carbonyl-metabolising enzymes in normal, immortalised and malignant human oral keratinocytes. Cell. Mol. Life Sci. 58, 1719–1726.
11 Oates, P. (2002) Polyol pathway and diabetic peripheral neuropathy. Int. Rev. Neurobiol. 50, 325–392.
12 Johansson, K., El-Ahmad, M., Kaiser, C., Jörnvall, H., Eklund, H., Höög, J.-O. and Ramaswamy, S. (2001) Crystal structure of sorbitol dehydrogenase. Chem. Biol. Interact. 130–132, 351–358.
13 Pauly, T.A., Ekstrom, J.L., Beebe, D.A., Chrunyk, B., Cunningham, D., Griffor, M., Kamath, A., Lee, S.E., Madura, R., Mcguire, D., Subashi, T., Wasilko, D. et al. (2003) X-ray crystallographic and kinetic studies of human sorbitol dehydrogenase. Structure 11, 1071–1085.

14 Ryde, U. (1996) The coordination chemistry of the structural zinc ion in alcohol dehydrogenase studied by *ab initio* quantum chemical calculations. Eur. Biophys. J. 24, 213–221.
15 Jelokovà, J., Karlsson, C., Estonius, M., Jörnvall, H. and Höög, J.-O. (1994) Features of structural zinc in mammalian alcohol dehydrogenase. Site-directed mutagenesis of the zinc ligands. Eur. J. Biochem. 225, 1015–1019.
16 Prozorovski, V., Krook, M., Atrian, S., Gonzàlez-Duarte, R. and Jörnvall, H. (1992) Identification of reactive tyrosine residues in cysteine-reactive dehydrogenases. Differences between liver sorbitol, liver alcohol and Drosophila alcohol dehydrogenases. FEBS Lett. 304, 46–50.
17 Banfield, M.J., Salvucci, M.E., Baker, E.N. and Smith, C.A. (2001) Crystal structure of the NADP(H)-dependent ketose reductase from *Bemisia argentifolii* at 2.3 Å resolution. J. Mol. Biol. 306, 239–250.
18 Karlsson, C. and Höög, J.-O. (1993) Zinc coordination in mammalian sorbitol dehydrogenase. Replacement of putative zinc ligands by site-directed mutagenesis. Eur. J. Biochem. 216, 103–107.
19 Roblick, U.J., Hirschberg, D., Habermann, J.K., Palmberg, C., Becker, S., Kruger, S., Gustafsson, M., Bruch, H.P., Franzén, B., Ried, T., Bergman, T., Auer, G. and Jörnvall, H. (2004) Sequential proteome alterations during genesis and progression of colon cancer. Cell. Mol. Life Sci. 61, 1246–1255.
20 Wilkins, M.R., Lindskog, I., Gasteiger, E., Bairoch, A., Sanchez, J.C., Hochstrasser, D.F. and Appel, R.D. (1997). Detailed peptide characterization using PEPTIDEMASS – A World-Wide-Web-accessible tool. Electrophoresis 18, 403–408.
21 Abagyan, R.A. and Totrov, M.M. (1994) Biased probability Monte Carlo conformational searches and electrostatic calculations for peptides and proteins. J. Mol. Biol. 235, 983–1002.
22 Abagyan, R.A., Totrov, M.M. and Kuznetsov, D.N. (1994) ICM – A new method for protein modeling and design. Applications to docking and structure prediction from the distorted native conformation. J. Comp. Chem. 15, 488–506.
23 Nemethy, G., Gibson, K.D., Palmer, K.A., Yoon, C.N., Paterlini, G., Zagari, A., Rumsey, S. and Scheraga, H.A. (1992) Energy parameters in polypeptides. 10. Improved geometric parameters and nonbonded interactions for use in the ECEPP/3 algorithm, with application to proline-containing peptides. J. Phys. Chem. 96, 6472–6484.
24 Miller, S. (1989) The structure of interfaces between subunits of dimeric and tetrameric proteins. Protein Eng. 3, 77–83.
25 Bogin, O., Levin, I., Hacham, Y., Tel-Or, S., Peretz, M., Frolow, F. and Burstein, Y. (2002) Structural basis for the enhanced thermal stability of alcohol dehydrogenase mutants from the mesophilic bacterium *Clostridium beijerinckii:* Contribution of salt bridging. Protein Sci. 11, 2561–2574.
26 Schreiber, G. and Fersht, A.R. (1996) Rapid, electrostatic assisted, association of proteins. Nat. Struct. Biol. 3, 427–431.
27 Selzer, T. and Schreiber, G. (2001) New insights into the mechanism of protein-protein association. Proteins 45, 190–198.